a

ingegneria sismica

International Journal of Earthquake Engineering

Anno XLIII - Num. 2 - 2026

Effects of Heat Treatment and Oxidation on the Microstructure and Compressive Strength of Ti-6Al-4V Lattice Structures Prepared by SLM

Xinyi Wang[1] *and Kaiyu Luo*[1,*]

[1] School of Mechanical Engineering, Jiangsu University, Zhenjiang 212013, P.R. China

SUMMARY: *The property of titanium alloys can be promoted via heat processing by changing their micro structure. Nevertheless, Ti-6Al-4V lattice frameworks require a personalized method on account of their big specific surface area and the stress gathering at the lattice joint points. In this research work, we have carried out a comparison between air and vacuum heat processing for Ti-6Al-4V lattices which are made through selective laser melting (SLM). The influences of these handling methods on the micro structure and compression performance were researched. When we carry out the air heat treatment operation, there was one oxide layer that got formed. This layer has the significant effect of decreasing the compressive strength of the Ti-6Al-4V lattices. In addition, the hardened α-Ti which is under the oxide layer caused a change from ductile fracture to brittle fracture and reduced the energy-absorption capacity. From another aspect, the vacuum heat treating has mitigated the damage which is related to oxidation. It also gave help to the formation of a lamellar inner micro structure, which thus contributed to stable deformation and a promoted energy-absorption capability. According to these results, it can be seen that vacuum heat handling is a more suitable approach for improving the micro structure and compression property of SLM-manufactured Ti-6Al-4V lattice frameworks.*

KEYWORDS: *lattice structure, selective laser melting, Ti-6Al-4V, heat treatment*

1 Introduction

Lattice materials are applied in aerospace, automotive, and biomedical engineering because of their outstanding specific strength and energy-absorbing abilities [1-4]. Selective Laser Melting (SLM) makes metal powder be able to complete rapid melting and solidification, hence obtaining components with metallurgical bonding and complex shapes [5-7]. Ti-6Al-4V is a kind of material which unites high specific strength together with favorable mechanical properties, and it is extensively applied in the medical and aerospace domains [8, 9]. Therefore, Ti-6Al-4V lattice structures which are manufactured through SLM are highly suitable for lightweight energy-absorbing components [10-12]. Nevertheless, these structures possess a big surface area, which therefore causes them to be easy to get surface flaws such as half-melted grains and fissures. These surface flaws lead to a lowering of compressive strength and a worsening of energy-absorption property [13-15]. In addition, the fast heat cycle that has relation with SLM produces a large quantity of acicular α/α′ and β phases. This result brings about limited ductility and unsteady compression performance [16, 17].

The traditional methods of after-processing, which contain machining, shot blasting and electrochemical processing, have the ability to promote surface strength. Nevertheless, their

*kyluo@ujs.edu.cn

https://doi.org/10.65102/is2026959

Published: 30 April, 2026

utilization within lattice structures brings forward problems, and therefore they possess the danger of bringing about destruction to thin supporting rods [18-20]. The processing of heating is a relatively more feasible choice. It may transform the α′ martensite which is produced in selective laser melting (SLM) into a more stable α + β structure, hence it promotes the mechanical performances of the material [21-25]. The researches which have been done before have proven many important results. As an example, in TC4 alloy which is processed by SLM, the temperature of heat-treatment may control the lamellar micro construction and micro hardness. In the Ti-6Al-4V alloy, the solution-aging processing methods are able to reduce the anisotropy. Furthermore, the processing of heating can promote the plastic deformation properties of TC31 lattice structures. More researches on Ti64 have further discovered that the dissolving temperature and holding duration possess an obvious influence on phase distribution, especially in the β phase and element transition areas.

The atmosphere which exists in the process of heat treatment possesses very important significance. When titanium alloys undergo heating in the air environment, they have the tendency to be oxidized. This oxidizing action brings about the generation of fragile oxide films which possess bad adhesive capacity toward the surface. After this, cracking and spalling may happen, which therefore can cause the worsening of the mechanical characteristics [29-31]. By comparison, the vacuum heat processing can remove the oxidation which air brings about. Furthermore, it is able to carry out modification upon grain morphology, and hence promote the transformational process that converts α′ into α + β. Regarding Ti-6Al-4V lattice structures which are manufactured through the method of selective laser melting (SLM), there is the necessity to conduct joint assessment on the influences of temperature, cooling rate, and atmosphere.

This research carries out a comparison work of atmospheric and vacuum heat-treatment craftworks for Ti-6Al-4V lattice structures which are made through Selective Laser Melting (SLM). For the purpose of describing the changing process of phases and microstructures, X - ray Diffraction (XRD), Optical Microscopy (OM), and Scanning Electron Microscopy (SEM) are utilized by us. At the same time, experiments of compression are employed by researchers to evaluate the mechanical property performance. In addition, this research carries out deep exploration on the atmospheric oxidation behavior. It also builds connections between the changes of microstructure, compressive reactions and the enhancement mechanisms.

2 Methods

2.1 Materials of Ti-6Al-4V Alloy and the SLM Process

Powder of Ti-6Al-4V titanium alloy, produced by gas atomisation and supplied by AVIMETAL AM, was used as the raw material. As shown in Figure 1(a), the morphology distribution of Ti-6Al-4V powder consists mainly of spheres and a small amount of irregular shapes. The distribution of the particle size of the powder particles is relatively concentrated in the range of 15-53 μm, and the mean particle size is 36.9 μm, as shown in Figure 1(b). The Chemical Composition of the Powder is as follows: Table 1

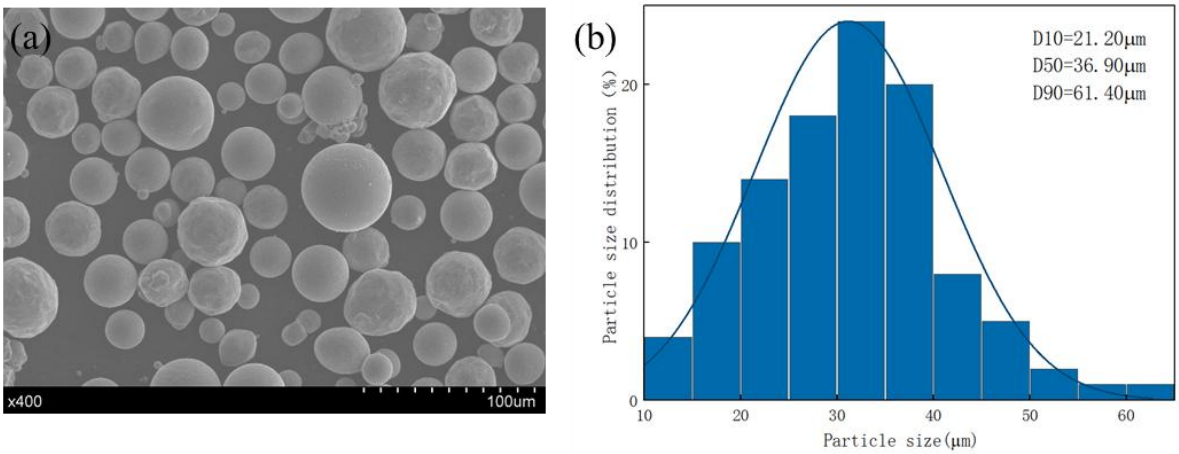

Figure 1: (a) SEM image of Ti-6Al-4V powder and (b) particle size distribution of the powder particles.

Table 1: Chemical Composition of Ti-6Al-4V.

Element	C	O	N	H	Ti	Al	V	Fe
Content(wt.%)	0.009	0.097	0.005	0.001	Bal.	5.97	3.83	0.037

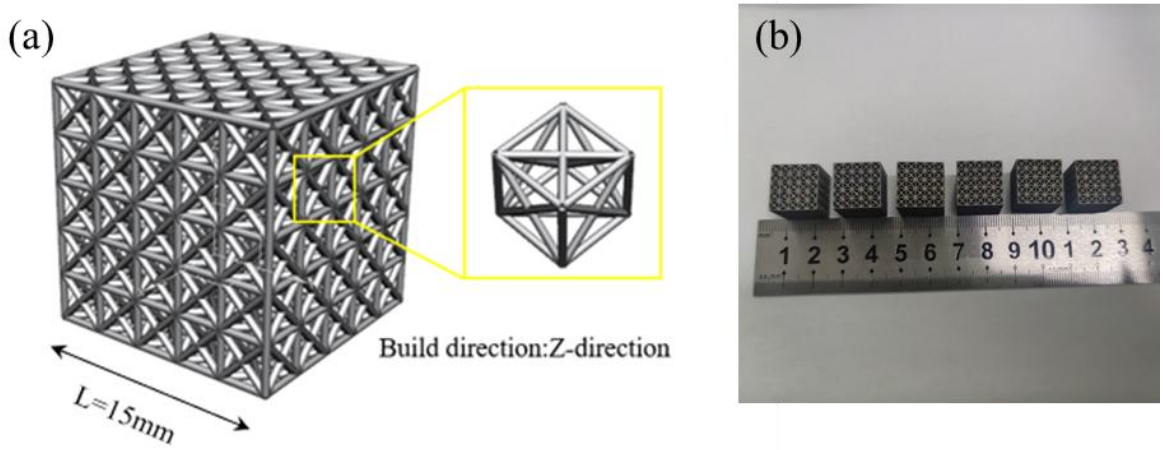

Figue 2: (a) CAD model of the lattice structure and (b) fabricated lattice structures.

Table 2: SLM Processing Parameters in This Study.

Manufacturing parameters	Value
laser power(W)	200,225,250
scanning speed(mm/s)	1000,1200,1400
scanning spacing(μm)	60
spot diameter(μm)	60
layer thickness(μm)	50
interlayer rotation(°)	50

Samples with a face - centered cubic (FCC) lattice structure were produced using the DiMetal - 650 selective laser melting (SLM) device. This device offers a maximum build

volume of 625 mm × 625 mm × 1100 mm. As depicted in Figure 2, the lattice featured struts with a thickness of 0.5 mm and had an overall size of 15 mm × 15 mm × 15 mm upon completion.Following the optimization of parameters, the SLM manufacturing process employed a laser power of 225 W, a scanning speed of 1400 mm/s, a hatch spacing of 60 μm, a spot diameter of 60 μm, a layer thickness of 50 μm, and an inter - layer rotation angle of 50°. These parameters were validated to guarantee the dimensional and structural precision of the lattice.

2.2 Heat Treatment Process

We divided the test specimens into three different groups, each of which includes four samples that possess a grid construction. One group was kept in its original condition after factory production, therefore it did not go through any heat-treatment procedures. The leftover two groups were processed by different heat-treatment methods which are as follows. The first heat-treatment method was carried out inside a muffle furnace in an air atmosphere. Our experiment put the samples into corundum crucibles, after that we put them into the muffle furnace. These samples were heated with a speed which is 10 °C each minute until they arrive at the target experiment temperature which is 920 °C. After this temperature was got, they were kept holding at 920 °C for a total of 2 hours. After that step, the samples were placed to cool inside the furnace until they arrived at room temperature. After that step, they were heated again to 560 °C, kept at this temperature for 4 hours, and finally cooled inside the furnace to room temperature one more time. The second method has contained a vacuum heat-treatment procedure which uses a vacuum furnace (Specnow VF1218H). We put the samples into an environment of vacuum (bar). They afterwards were put under same temperature and time parameters as what was in the first method, and were cooled through furnace to room temperature.

2.3 Microstructure Characterization and Compression Testing

The specimens were first abraded using sandpapers with grits of 400, 800, 1200, and 2000. Subsequently, they were buffed with a 2.5 - micrometer diamond suspension. After that, the samples were etched for 15 seconds with Keller’s reagent, which consisted of 5 milliliters of nitric acid (HNO_3), 2.5 milliliters of hydrofluoric acid (HF), and 50 milliliters of water (H_2O).The micro - structures, oxidized surfaces, and cross - sectional oxide layers were inspected using an optical microscope (OM, Observer Z1m) and a scanning electron microscope (SEM, JSM - 7800F). The phase composition was analyzed via X - ray diffraction (XRD, SmartLab) within the range of 20° to 80° at a scanning rate of 2° per minute. The elemental distribution was determined by energy - dispersive X - ray spectroscopy (EDS).Compression tests were carried out in accordance with the GB/T 7314 - 2017 standard using a Shimadzu AGS - X100KN testing machine. Quasi - static compression was conducted along the selective laser melting (SLM) build direction at a speed of 1 millimeter per minute at room temperature. The load and axial strain were registered by the built - in load cell and laser extensometer. The tests were terminated when the compressive strain reached 60%. The energy absorption was computed from the area under the stress–strain curve, and each testing condition was replicated three times.

3 Result

3.1 Phase Analysis

The XRD patterns of the as-built and heat-treated Ti-6Al-4V lattice structure samples are shown in Figure 3. Based on the above data, the as-built Ti-6Al-4V samples mainly contained the α/α'-Ti and β-Ti phases. After heat treatment in an air atmosphere, distinct diffraction peaks of TiO_2 and Al_2O_3 were observed; the intensity of the TiO_2 peaks was significantly higher than that of the Al_2O_3 peaks, indicating that a TiO_2 -dominant oxide layer had been formed with a small amount of Al_2O_3. All of the heat-treated samples showed an increase in the diffraction peak intensity of β-Ti, and this was due to element redistribution in the β-phase region during solution treatment and β-phase precipitation induced by aging treatment. In addition, the diffraction peaks of α/α'-Ti shifted slightly to lower angles after heat treatment; thus, it can be concluded that the heat-treatment process induced the conversion of metastable α' martensite into the stable $\alpha + \beta$ phase.

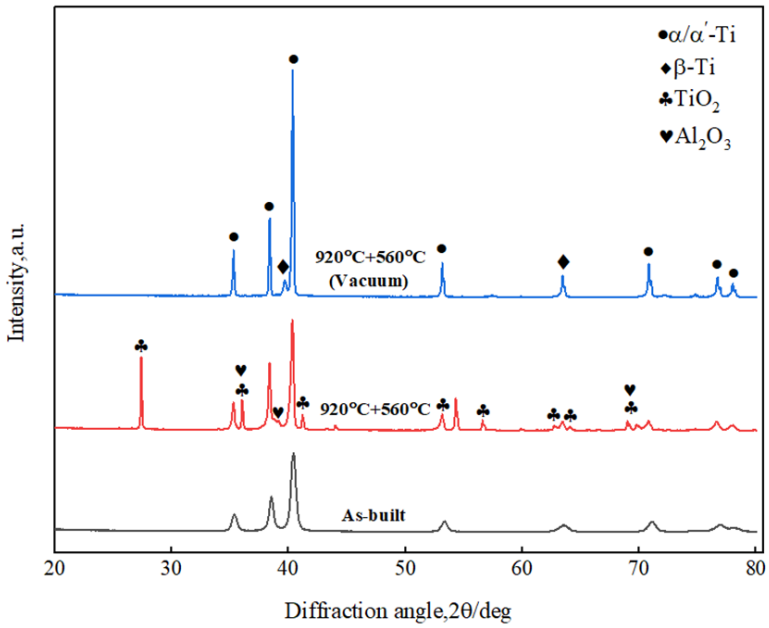

Figure 3: XRD Patterns of the Ti-6Al-4V Lattice Structure in As-built and Heat-treated States.

3.2 Microstructure Characterization

Figure 4 presents scanning electron microscopy (SEM) images of the surfaces of the as - fabricated and heat - treated lattice structure specimens. In Figure 4(a), it can be observed that a significant quantity of unmelted or partially melted metal powder particles are adhering to the surfaces of the columns in the as - fabricated specimen.During the selective laser melting procedure, the energy at the surface of the molten pool diminishes rapidly, while the internal energy stays at a high level. Consequently, after cooling, a portion of the liquid metal is ejected and forms spherical particles on the surface. [32, 33]. Spherical particles attached to the pillars increase the diameter of the pillars, and thus the actual diameter of the sample pillars is larger than the design value. The other is that the spherical particles on the surface may cause stress concentration at the pillars. As shown in Figure 4(b), there is obvious oxidation at the surface of the sample after heat treatment in air, and a layer of large-grained oxides has been formed on the surface of the sample. As shown in Figure 4(c), after vacuum

heat treatment, the sintering gap between the unmelted powder and the pillars has widened, and the number of metal powder particles on the pillar surface has been significantly reduced.

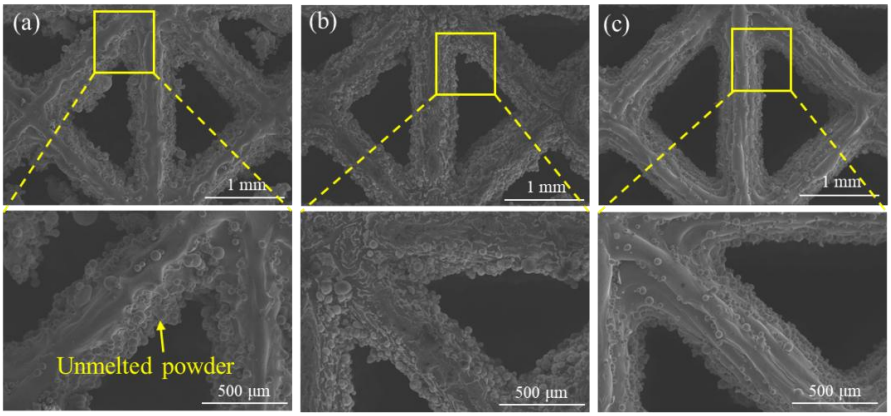

Figure 4: SEM images of the Ti-6Al-4V lattice structure in the as-built and heat-treated states: (a) As-built, (b) 920 °C + 560 °C, (c) 920 °C + 560 °C (Vacuum).

The cross-section micro-structures of the as-manufactured, air-handled, and vacuum-handled lattice samples are compared in Figure 5 and Figure 6. In all situations, the support rods are composed of bright α/α′-Ti regions and dark β-Ti regions. The finished after-construction specimens show the feature Selective Laser Melting (SLM) micro structure. This micro structure is mainly constituted by stretched first α/α′-Ti together with a small amount of β-Ti, and also holes brought by argon and not regular melted cavities [34, 35]. After we have carried out heat treatment, the inner microstructures of the samples handled by air and handled by vacuum are similar. The main primary α/α′-Ti phase becomes more thick, and the starting acicular α′ martensite is for the most part changed into an α + β lamellar structure. When β-Ti is separated out under high temperature conditions, the stretched α/α′-Ti is divided. Its percentage goes down, and it by degrees obtains a short-rod form or turns into partly spheroidized. Correspondingly, the proportion of β-Ti has an increase, this circumstance accords with the X-ray Diffraction (XRD) results. The main difference can be observed on the surface. The processing of air heat causes that a clear oxide layer is formed on the struts. This layer maintains its continuity, yet it possesses internal pores and cracks.

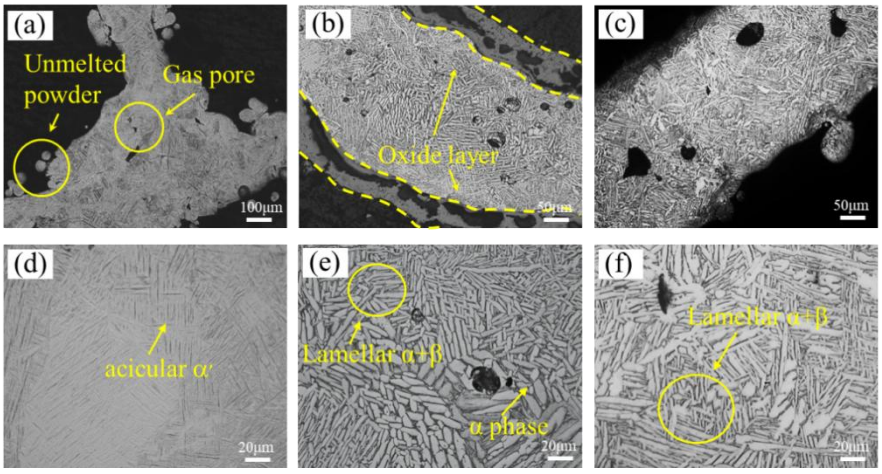

Figure 5: OM images of the Ti-6Al-4V lattice structure in the as-built and heat-treated states: (a,d) As-built, (b,e) 920 °C + 560 °C, (c,f) 920 °C + 560 °C (Vacuum).

Microscopic structure analysis via SEM shows that, after heat treatment, the β phase nucleates at the boundaries of the acicular martensitic α' phase (Figs. 6(b) and (c)). Given that α' is supersaturated with V and the β phase has a higher capacity to dissolve V than the α phase, V begins to diffuse fromα' to the β phase. Therefore, a decrease in the V content of α' occurs, and thus α' gradually transforms into the α phase. The original acicular martensitic α' phase has almost entirely transformed into a lamellar mixed structure of the α' phase and the β phase.

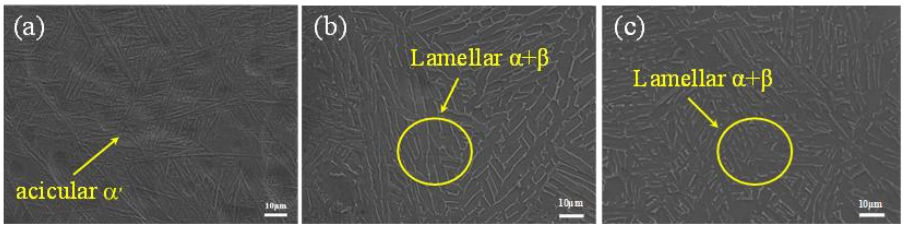

Figure 6: SEM images of the lattice structure in the as-built and heat-treated conditions: (a) As-built, (b) 920 °C + 560 °C, (c) 920 °C + 560 °C (Vacuum).

We have carried out Energy-dispersive X-ray spectroscopy (EDS) analysis on cross-sections of the as-made and heat-treated lattice structure samples. This analysis has furthermore discovered the micro structure changes which are brought by the two heat processing methods. The result of the EDS surface scanning is displayed in Figure 7. Just like what Figure 7(b) shows, regarding the specimen that has got heat treatment in air, the oxide layer on surface possesses many pores, fissures, and delaminations. We can observe that continuous horizontal cracks exist at the interface which is between oxide layer and substrate. The element distribution diagrams are utilized by us for the illustrating of the structure of oxide layers. The oxide has already come apart in layers, and the most outer portion of this oxide layer holds a high percentage of aluminum.

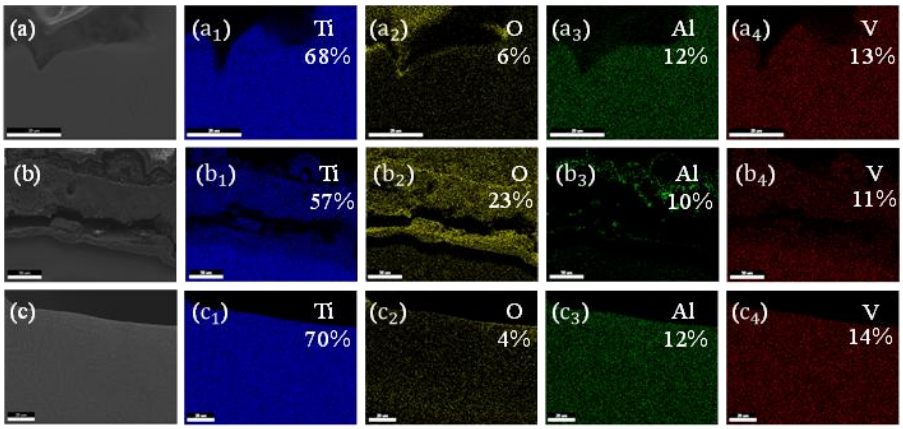

Figure 7: EDS surface scanning analysis of the cross-sectional morphology of the lattice structures in the as-built and heat-treated states: (a) As-built, (b) 920 °C + 560 °C, (c) 920 °C + 560 °C (Vacuum).

EDS line scanning analysis was performed on the cross-section of the sample to observe the oxidation state further (Figure 8). As shown in Figures 8(a) and 8(d), the oxygen atoms in the as-built specimens are uniformly distributed and do not accumulate at the surface; thus, it can be concluded that there has been no surface oxidation of the as-built specimens. Figures 8(b) and 8(e) show that there is an oxygen-rich layer at the top of the air-heated samples. Ti

and Al diffuse outwards, and O diffuses inwards; both are clearly visible. Oxygen-rich regions are at the top and have an oxide layer of about 40 μm thick. The oxides here are mainly composed of TiO and Al_2O_3. Elemental mapping of the oxide layer shows that the peaks for Al and Ti occur alternately. TiO_2 is generated by oxidation at this time. As the oxidation degree increases, the structure of the oxide layer is modified; at the same time, there is an enrichment of Al and the alternating formation of Al_2O_3 and TiO_2 layers. Transverse cracks can be seen between the oxide film and the substrate, and the oxide film has detached from the substrate. At the same time, many cracks, pores and delaminations can also be found in the oxide scale. Local stress concentration will occur near these cracks and pores; as a result, the damage caused by the compression force will be relatively concentrated in this area and lead to premature failure of the structure. Oxygen can also be admitted through the cracks and will continue to disperse within the matrix. Dissolution of oxygen in the substrate will induce the formation of a hardened α-Ti layer under the oxide scale and reduce the toughness of the struts. As shown in Figures 8(c) and 8(f), there is a slight enrichment of oxygen atoms at the surface of the vacuum-heat-treated samples. This is because there will be residual air in the quartz tube during heating for heat treatment, and thus slight oxidation will occur at the surface. Oxygen atoms are uniformly distributed in the samples, and no oxides have formed.

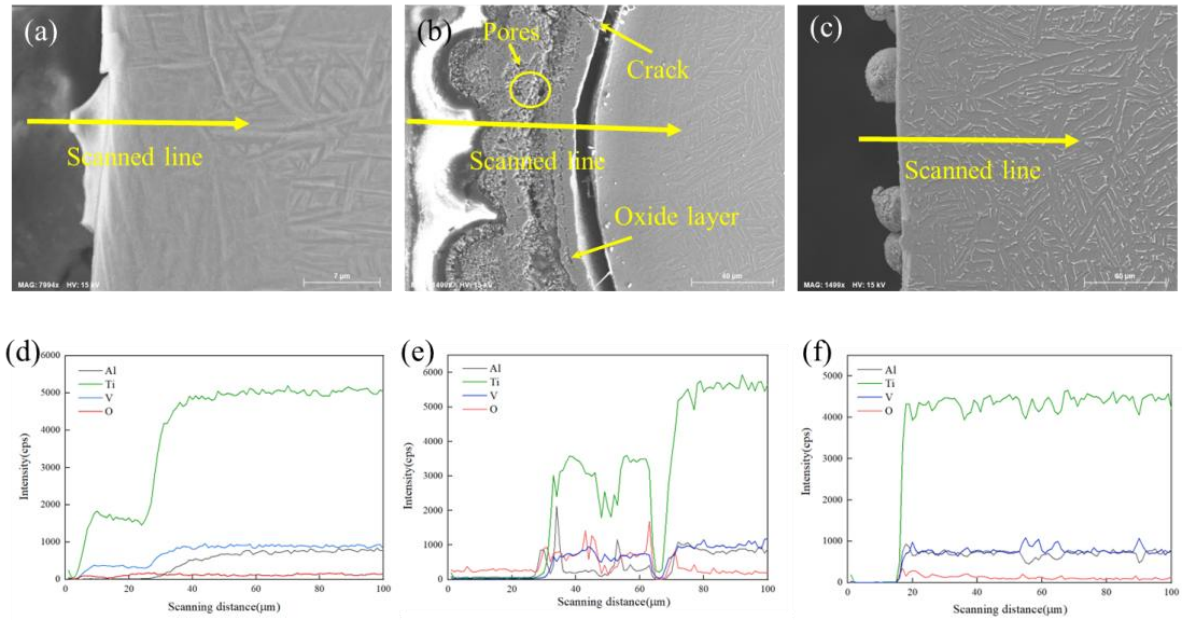

Figure 8: EDS line scanning analysis of the cross-sectional morphology of the Ti-6Al-4V lattice structure in the as-built and heat-treated states: (a,d) As-built, (b,e) 920 °C + 560 °C, (c,f) 920 °C + 560 °C (Vacuum).

3.3 Compressive properties

Figure 9 gives a comparison of the nearly static compression features of lattice structures under many different heat-treatment situations. Just like what is shown in Figure 9(a), all stress–strain diagrams are composed of three clear phases. The starting stage is the linear elastic stage. In this period, pressure increases hand in hand with tension. The elastic modulus may be obtained from the gradient of the fitting straight line, and the yield strength hence is defined as the 0.2% offset stress. The second stage is the plastic platform period. After we arrive at the plateau stress, the stress does fluctuation around a nearly invariable value. The third stage is the compacting time period, which is featured by repeated stress maximum values. These peak appearances are the outcome of the lattice that carries out layer-by-layer

collapse. The atmosphere of heat-treatment possesses a quite remarkable influence upon the compression performance. The samples which have been treated in air display poorer mechanical performance when we compare them with the as-built samples. A comparatively obvious stress decrease that exists in the samples which have been treated by air, it indicates structural failure. On the opposite side, samples which have been processed in a vacuum keep stress–strain curves that are more close to those of the as-built samples, hence it implies that compressive deformation is more stable.

The stress-strain curves which are shown in Fig. 9(b) can be utilized by researchers to get the plateau stress, elastic modulus, and yield strength of both the as-built and the heat-treated lattice structures. Regarding the lattice structures which have been undergone heat treatment in air, all three of these mechanical target indices are markedly lower than those of the specimens which are as they were after being constructed. By comparison, the plateau stress of the lattice structure which has experienced vacuum heat-treatment displays comparatively small change when compared to the plateau stress of the as-built samples. When make comparison with the as-constructed test pieces, the maximum increments of the average numerical values of the elastic modulus and yield strength for the vacuum heat-treated lattice structures are 4.6% and 15% respectively. From the foregoing content, it may clearly be seen that oxidation can greatly reduce the mechanical performances of SLM Ti-6Al-4V lattice structural bodies.

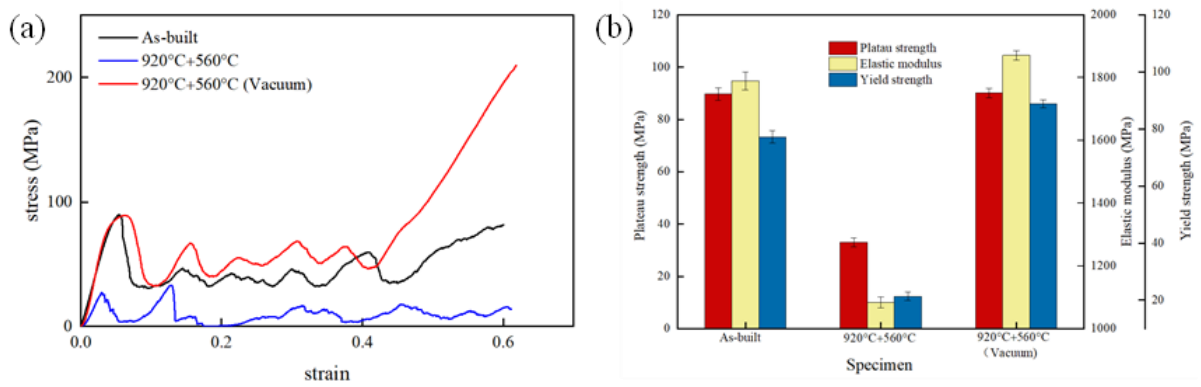

Figure 9: Compressive Properties of the Ti-6Al-4V Lattice Structure in the As-built and Heat-treated States: (a) Compressive Stress-Strain Curves and (b) Plateau Strength, Elastic Modulus and Yield Strength.

The lattice structure possesses the capability to absorb energy through the deformation of compression. To both the as-manufactured and heat-processed lattice frame structures, the specific energy absorption (SEA) and energy absorption (EA) curves under quasi-static load have been calculated. The specific energy absorb, which is also called the specific energy absorb ability, is the energy that is absorbed by each unit mass of one structure. This norm acts as one of the representative measures for assessing the energy-absorbing capability of one structure. The SEA of one structure shows the amount of energy which is absorbed when the structure is undergone external impact and compression. This tool possesses the especial effectiveness for the manifestation of the energy-absorbing capability that lattice structural frameworks have [37, 38]. The calculation of SEA can be carried out by utilizing the formula which is given in[39].

$$SEA=\frac{EA}{M}$$

M is the mass of the structure here. Energy absorption (EA) is the total energy lost by a structure due to plastic deformation, which can be obtained as the area under the stress-strain curve.

$$EA=\int_0^{\delta} F(x)dx$$

In the formula，δ represents strain; $F(x)$ represents the magnitude of the stress variation of the structure with strain. Figure 10 gives a summation of energy absorption (EA) and specific energy absorption (SEA). Along with the advancement of strain, the capability of energy absorption has an increase. But, the method of heat treatment possesses a remarkable influence on the performance. Lattices which have accepted air processing display lower EA and SEA numerical values when compared with specimens in their original as-manufactured condition. This is because the fact that surface oxides have a restriction upon the ability of plastic deformation. From another aspect, vacuum heat processing can increase the absorption of energy. It realizes this thing through making the fine microstructure better and helping bigger plastic deformation to happen in the process that compression carries on.

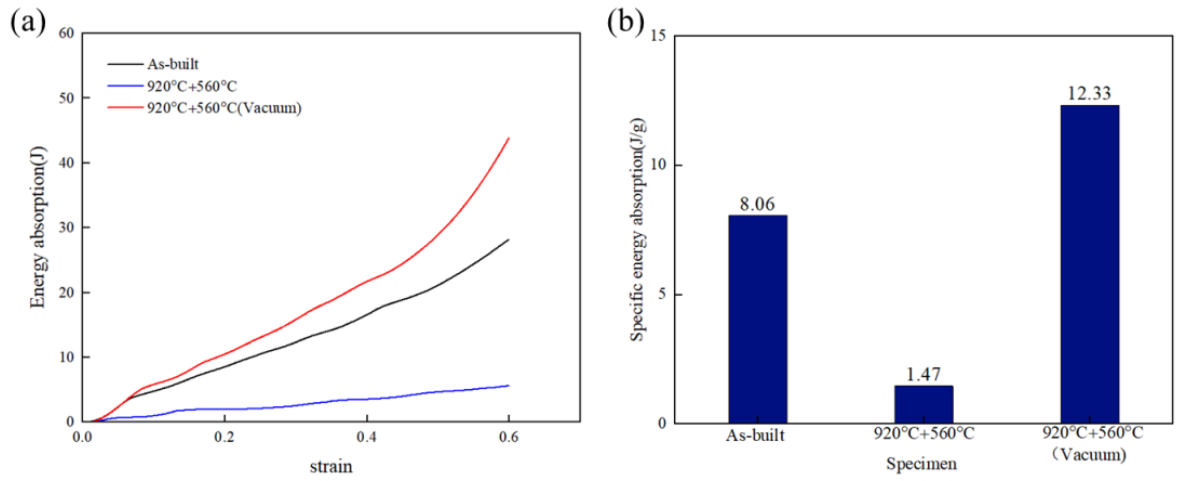

Figure 10: Energy Absorption Properties of Ti-6Al-4V Lattice Structure in the As-built and Heat-treated States: (a) Energy Absorption-Strain Curves and (b) Specific Energy Absorption.

Fig. 11 is the compressive deformation behaviour of the as-built and heat-treated lattice structure in a quasi-static compression test. It can be seen from the above that under the effect of compressive loads, the as-built samples mainly show a layer-by-layer collapse failure mode. At this time, a pattern of stress will be established in the lattice structure after plastic deformation. An increase in strain causes a shear failure of the lattice structure at a diagonal. The shear band originates at the bottom-left corner and runs to the upper-right corner. Due to the ongoing effect of compressive forces, both the upper and lower parts of the lattice structure are compressed and finally yield in a denser state. In the air environment, the heat-treated lattice structure undergoes diagonal shear failure in the lower right corner of the sample at the beginning of the strain. A shear crack has formed in the lattice structure, and as a result, the entire structure has fallen over suddenly. Under continuous application of compressive load, the pillars of the lattice structure break and fracture; thus, the entire structure fails and the lattice structure is completely destroyed. The vacuum heat-treated lattice structure shows a layer-by-layer collapse failure mode under all compression loading. No diagonal shear cracks have been formed. With an increase in stress, each layer of the

lattice begins to densify under the effect of compression; the deformation of the structure accumulates in layers, and finally, the structure fails. That is to say, compared with the two previous samples, vacuum heat treatment reduces the problem of stress concentration at the nodes of the lattice structure pillars during compression to a certain extent, lowers the transfer of shear stress to the diagonal pillars, and enables the lattice structure to bear larger strain and absorb more energy.

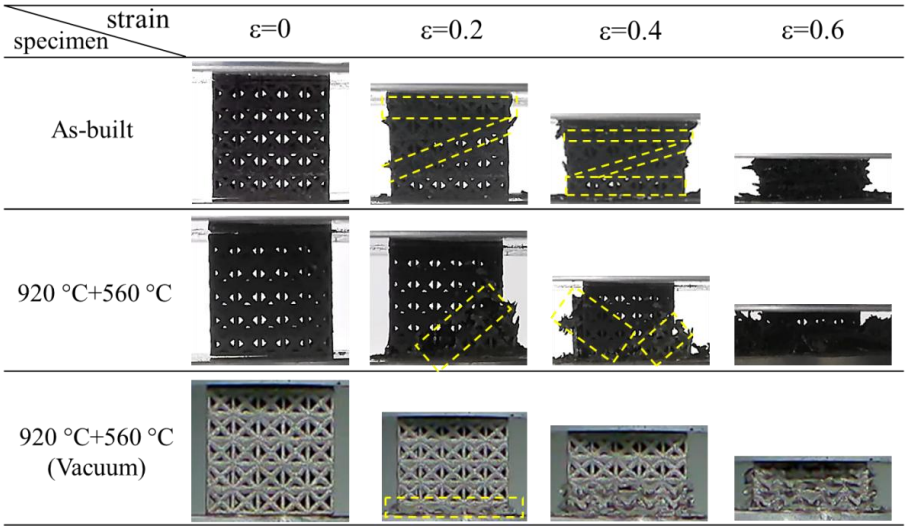

Figure 11: Compressive deformation behaviour of Ti-6Al-4V lattice structure in the as-built and heat-treated states under quasi-static compression test.

3.4 Fracture Morphology

Figure 12 has drawn a scheme of the compression crack shape of the as-constructed and heat-processed grid frameworks. In Figure 12(a), the fracture surface of the as-manufactured lattice structure shows comparatively uniform. People are able to observe some big empty spaces and not melted particles on this broken face. These characteristic positions can become stress gathering places, and therefore thus become the starting places of cracks. When we do observation under high multiple enlargement, the broken face shows that there exist some shallow concave places and stepped split planes. Therefore, it can hence be inferred that the mechanism of compression fracture follows a brittle-ductile combined fracture mode. Turning next to Figure 12(b), the fracture surface of the lattice structure which was heat-treated in air is more smooth when compared with the fracture surface of the as-built specimen. The main kind of fracture face is made up of step-shaped cleavage planes, which thus shows it is a brittle fracture. Furthermore, according to the above-mentioned figures, therefore it is obvious that the oxide layer on the surface of the struts has separated from the inner material. A porous oxide layer which is on the uppermost part of the strut can be the position from which cracks begin to generate. In the process of compressive loading, a local shear band which appears at an earlier time, therefore, can decrease the plasticity of this structure. Therefore, the whole structure has weaker robustness, hence its compressive bearing ability has reduction. At last, in Figure 12(c), uniform sunken marks can be observed through the whole fracture surface of the lattice structure which has been heat-treated in a vacuum. These sunken places show the features of a tenacity crack break. When we make a comparison with the as-built sample, the number of round pores on the fracture face of the vacuum heat-treated lattice structure, which is caused by powder that has not been molten, has a very obvious reduction. We also hold the anticipation that the strength of the specimens which are compressed in the test will

experience an increase.

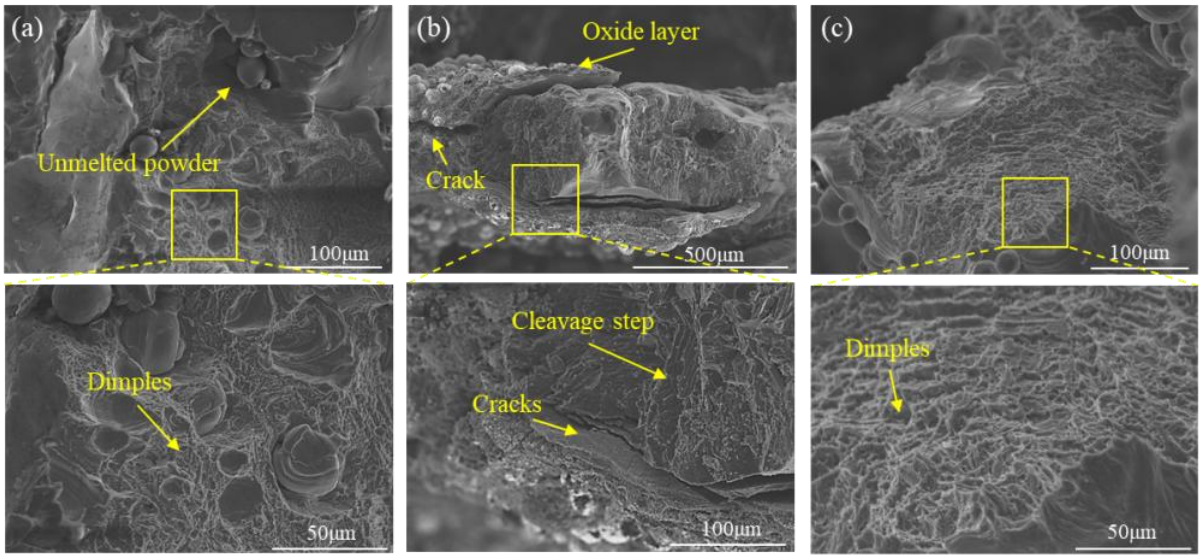

Figure 12: Compressive fracture morphology of the Ti-6Al-4V lattice structure in the as-built and heat-treated states. (a) As-built, (b) 920 °C + 560 °C, (c) 920 °C + 560 °C (Vacuum).

4 Discussion

4.1 Oxidation Mechanism

At this time, the growth of the oxide film can affect the mechanical properties of the SLM Ti-6Al-4V lattice structure significantly. Based on Figures 3 and 6, the two main chemical reactions that occur during the heat treatment of the Ti-6Al-4V lattice structure in air are as follows:

$$Ti+O_2=TiO_2$$

$$4Al+3O_2=2Al_2O_3$$

Figure 13 gives a description of the oxidation procedure of Ti-6Al-4V. When oxidation just begins, oxygen moves toward inside and reacts with titanium to produce titanium dioxide (TiO_2). This reaction brings about the generation of a zone adjacent to the oxide/substrate interface which has lost titanium and been increased in aluminum content. After that time, aluminum atoms diffuse to outside and generate aluminum oxide (Al_2O_3). Along with the oxidation proceeding forward, the aluminum is gradually consumed completely. After this situation occurs, titanium once again comes into contact with oxygen, hence it causes the generation of new TiO_2 layers. The alternate generation of Al_2O_3 and TiO_2 brings about a multi-layer oxidized covering on the surface of the alloy [40, 41]. When the oxide covering becomes thicker, because of growth stress and thermal stress, crack and peel off at the junction occur. The generating of the oxide brings into being a compressive growing stress. At the same time, in the course of cooling progress, thermal stress is produced on account of the difference in expansion between TiO_2, Al_2O_3, and Ti - 6Al - 4V. The thermal expansion coefficients of theirs are approximately 8.2×10^{-6}, 8.1×10^{-6}, and 10.8×10^{-6} $°C^{-1}$ separately. Because the base material has a bigger expansion degree than the oxide compounds, therefore, the compressive stress is gradually accumulated inside the oxide layer. This gathering of

stress brings about the production of pores, cracks, and the falling off of the oxide when cooling happens. The dissolving process of oxygen also leads to the fact that the hardened α-Ti layer which is under the coating becomes thicker. This kind of thickening can lower the plastic property of the supporting rods and hence make the behavior of fracture have more brittleness. These changes bring about a bad influence upon the mechanical characteristics of Ti-6Al-4V lattice frameworks. By comparison, the vacuum heat processing method can this oxidation-connected harm stop.

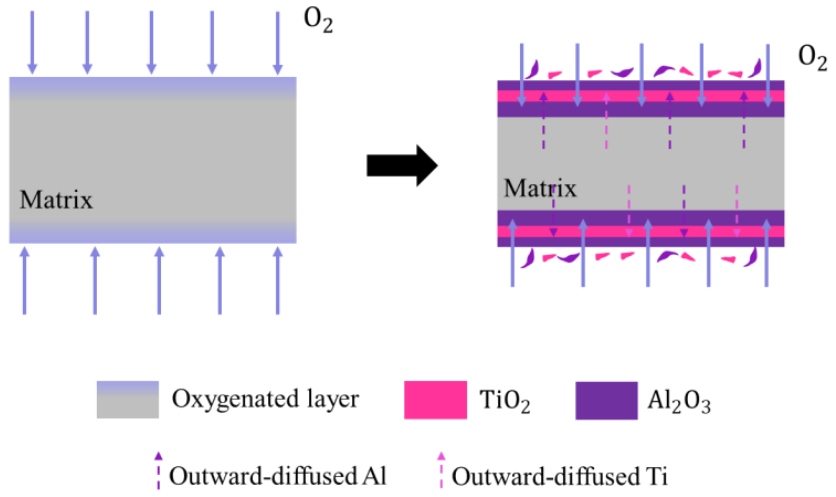

Figure 13: Oxidation Mechanism of Ti-6Al-4V Alloy

4.2 Compression fracture mechanisms related to the microstructure

The utilization of a heat-treatment process changes the micro-structure and the macroscopic support rod form of Selective Laser Melting (SLM) Ti-6Al-4V grid constructions, which as a result influences their pressure performance properties. Figure 14 has given the fracture shapes of Ti-6Al-4V lattice frameworks under pressure forces after two different heat-processing methods. There exists a very obvious difference in the compression intensity between grid structures which received heat treatment in the air and those which received heat treatment in the vacuum. This circumstance may be attributed to the big specific surface area that the high-porosity lattice structure has, which gives a relatively big area for the oxide layers to come into being. One comparatively loose, multi-layer oxide film has on the surface of the Ti-6Al-4V alloy structure evenly formed. In the process of compression, cracks and pores that exist in the oxide layer have the possibility to become the sites where cracks initiate. Under a low compression load, these cracks quickly extend into the inner part of the structure. This makes a number of struts have early failure, hence it destroys the completeness of the lattice structure, and hence finally leads to the quick failure of the whole structure [42, 43]. The stress concentration is the reason that makes the oxide layer get separated from the Ti-6Al-4V base body. Therefore, a local shear band has formation at the early time of the compression stage, hence the structure has fracture along this shear band. All these factors together cause that the compressive strength of this structure get a decrease.

Oxide-free vacuum heat treatment. The main reasons for the improvement in the mechanical properties of the studied Ti-6Al-4V lattice structures after heat treatment are an increase in the ductility of the struts. This is because, after heat treatment at a relatively high temperature, the size of the sintering neck between the unmelted powder particles and the lattice struts increases; thus, the elastic modulus also increases accordingly [5]. At the same time, due to a high cooling rate in the SLM process, acicular α' martensite forms in the

Ti-6Al-4V lattice structure at high temperatures. Martensite is then transformed into an $\alpha+\beta$ lamellar structure. In addition, the α lamellae have also coarsened significantly. Therefore, the plasticity is better than that of the as-built samples. After heat treatment, the lattice structure of Ti-6Al-4V in the solution-treated state is a rod-shaped primary α phase. After ageing treatment, the secondary α' phase is formed. The Ti-6Al-4V titanium alloy is in a diffusional phase transformation at the furnace cooling stage. The division of the component forms a two-phase system to enhance the ductility of the structure. The $\alpha+\beta$ lamellar structure that develops upon heating is relatively ductile. A relatively large increase in the size of grains will lead to an expansion of the separation distance between lamellae. These lamellar structures have different growth directions, and the grain boundaries cannot move along the axial direction of the α-lamellae; thus, the growth of grain boundaries is restricted and the energy absorption capacity is enhanced. The presence of the β phase and the high-density α/β phase boundaries inhibit crack propagation and thus enhance the compressive strength.

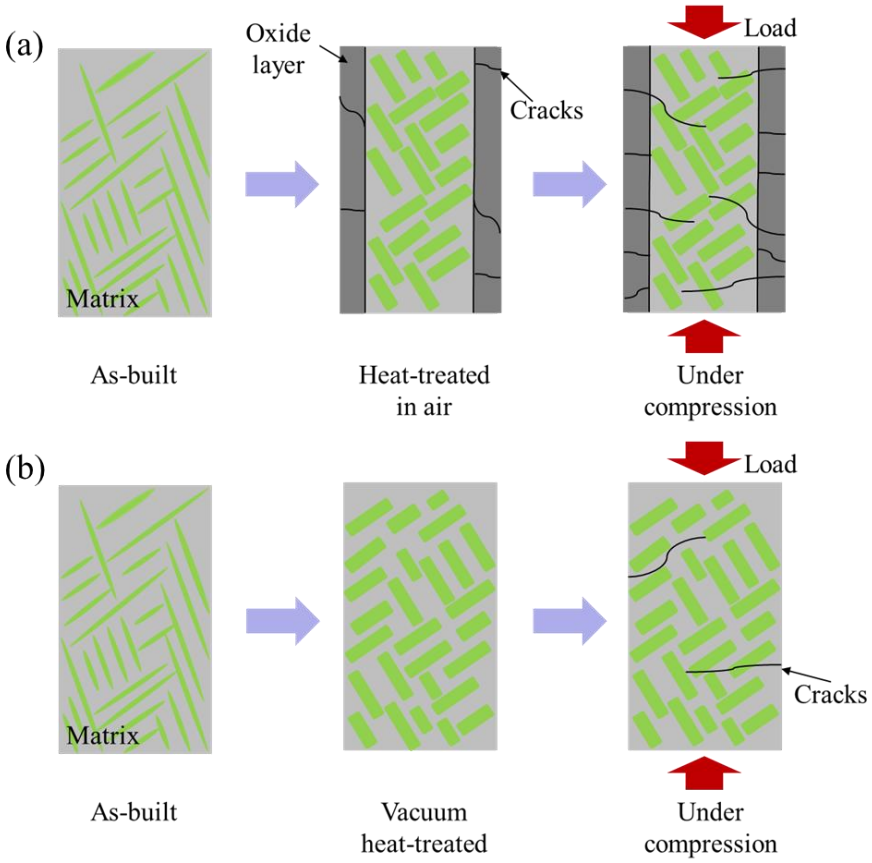

Figure 14: Schematic diagram of the cracking pattern of the strut under compressive load at different heat-treatment methods: (a) 920 °C + 560 °C, (b) 920 °C + 560 °C (Vacuum).

5 Conclusions

This research has carried out a comparison on air and vacuum heat treatments for Ti - 6Al - 4V lattice structures which are made through Selective Laser Melting (SLM), hence got the following results:

(1)The as-fabricated lattice structures have many not melted powder particles that attach

on the surfaces of the struts. The fast cooling course in SLM caused the coming into being of a great many long thin primary α/α′ - Ti phases. When compression is applied, the restricted motion of dislocations has facilitated the starting of cracks at the lattice points where the stress has been concentrated.

(2) The processing which uses heat has not caused the obvious changes of the appearance of crystal grains. The vacuum heat treatment made the quantity of brittle needle-shaped martensite become lower, and promoted the formation of a layered α + β structure. The more densely accumulated phase boundaries and the raised proportion of β-Ti thus promoted the ductility and energy-absorbing ability of this material.

(3) The oxidation which happens at high temperatures within air has led to a reduction of the compressive strength. The oxides which are on the surface brought about stress concentration and thus led to premature partial shear fractures. At the same time, the hardened α-Ti layer which is under the oxide layer has made the fracture behavior become more brittle and thus reduced the energy-absorbing ability.

(4) The shape of the broken part has given the evidence about the differences in mechanical properties. The after-manufacturing sample displayed shallow concave pits and fracture splitting surfaces, hence it indicates a mixed brittle-ductile breaking behavior. After the process of vacuum heat treatment, the fracture surface was mainly constituted by evenly distributed dimples, which hence indicates a ductile fracture. The energy absorbing capacity obtained a promotion of 53.0% when make comparison with the as-constructed specimen, therefore this result has proven that vacuum heat processing is able to effectively promote the mechanical behaviors of the lattice construction.

Author's Profile

Xinyi Wang was born in Luoyang, Henan Province, China in 2000. She is currently studying at the School of Mechanical Engineering, Jiangsu University, with her main research focus on additive manufacturing.

References

[1] Wang, D.-W., Wen, Z.-H., Glorieux, C., & Ma, L. (2020). Sound absorption of face-centered cubic sandwich structure with micro-perforations. Materials & Design, 186.

[2] Tancogne-Dejean, T., & Mohr, D. (2018). Stiffness and specific energy absorption of additively-manufactured metallic BCC metamaterials with tapered beams. International Journal of Mechanical Sciences, 141, 101-116.

[3] Yang, J., Chen, X., Sun, Y., Zhang, J., Feng, C., Wang, Y., et al. (2022). Compressive properties of bidirectionally graded lattice structures. Materials & Design, 218.

[4] Zhou, H., Zhang, X., Zeng, H., Yang, H., Lei, H., Li, X., et al. (2019). Lightweight structure of a phase-change thermal controller based on SLM-manufactured lattice cells. Chinese Journal of Aeronautics, 32(7), 1727-1732.

[5] Li, D., Qin, R., Xu, J., Chen, B., & Niu, X. (2022). Effect of heat treatment on AlSi10Mg lattice structure manufactured by selective laser melting: Microstructure evolution and compression properties. Materials Characterisation, 187.

[6] Ghouse, S., Oosterbeek, R. N., Mehmood, A. T., Vecchiato, F., Dye, D., & Jeffers, J. R. T. (2021). Vacuum heat treatment of titanium porous structures. Additive Manufacturing, 47.

[7] Herzog, D., Seyda, V., Wycisk, E., & Emmelmann, C. (2016). Additive manufacturing of metals. Acta Materialia, 117, 371-392.

[8] Ke, X., Zhang, J., Cai, W., Xu, S., Deng, S., Liu, Q., et al. (2024). Microstructure evolution and oxidation mechanism of TA5 titanium alloy during high-temperature heat treatment. Vacuum, 227.

[9] Sarraf, M., Rezvani Ghomi, E., Alipour, S., Ramakrishna, S., & Sukiman, N. L. (2021). A state-of-the-art review of fabrication and properties of titanium and its alloys for biomedical applications. Bio-Design and Manufacturing, 5(2), 371-395.

[10] Maconachie, T., Leary, M., Lozanovski, B., Zhang, X., Qian, M., Faruque, O., et al. (2019). SLM lattice structures: Characteristics, performance and applications. Materials & Design, 183.

[11] Ge, J., Huang, J., Lei, Y., O'Reilly, P., Ahmed, M., Zhang, C., et al. (2020). Microstructural features and compressive strength of SLM Ti-6Al-4V lattice structures. Surface and Coatings Technology, 403.

[12] Khanna, P., Sood, S., Mishra, P., Bharadwaj, V., Aggarwal, A., & Singh, S. J. (2024). Analysis of compression and energy absorption behavior of SLM printed AlSi10Mg triply periodic minimal surface lattice structures. Structures, 64.

[13] Ma, S., Zhu, R., Yang, S., Yang, Q., Wei, K., & Qu, Z. (2024). Influence of geometric imperfections on the mechanical behaviour of Invar 36 alloy lattice structures fabricated by selective laser melting. International Journal of Mechanical Sciences, 274.

[14] Vrána, R., Jaroš, J., Koutný, D., Nosek, J., Zikmund, T., Kaiser, J., et al. (2022). Contour laser strategy and its advantages for lattice structure manufacturing in selective laser melting technology. Journal of Manufacturing Processes, 74, 640-657.

[15] Du, Y., He, K., Guo, R., Zhou, Z., Ming, G., Liu, Q., et al. (2025). Mechanical properties of CoCrFeMnNi high entropy alloy lattice structures formed by selective laser melting. Materials & Design, 252.

[16] Wang, C., Xu, N., Zhang, G., Xu, G., & Xing, F. (2024). Effect of heat treatment on microstructure and properties of vacuum laser-welded Ti-6Al-4V titanium alloy. Journal of Materials Research and Technology, 30, 6309-6320.

[17] Wu, G. Q., Shi, C. L., Sha, W., Sha, A. X., & Jiang, H. R. (2013). Effect of microstructure on fatigue properties of Ti–6Al–4V titanium alloys. Materials & Design, 46, 668-674.

[18] Bagehorn, S., Wehr, J., & Maier, H. J. (2017). Application of mechanical surface finishing processes for roughness reduction and fatigue improvement of additively manufactured Ti-6Al-4V parts. International Journal of Fatigue, 102, 135-142.

[19] Ullah, I., Zhang, S., & Waqar, S. (2022). Numerical and experimental investigation of thermo-mechanically induced residual stresses in high-speed milling of Ti-6Al-4V alloy. Journal of Manufacturing Processes, 76, 575-587.

[20] Zhang, Y., Li, J., Che, S., & Tian, Y. (2019). Electrochemical polishing of additively manufactured Ti–6Al–4V alloy. Metals and Materials International, 26(6), 783-792.

[21] Zhang, J., Yang, P., Yang, H., Yang, W., Yang, K., & Xu, W. (2025). Effect of heat treatment on microstructure and properties of hybrid manufacturing TC4 alloy bonding zone. Journal of Materials Research and Technology, 34, 1108-1119.

[22] Yang, W., Chen, Y., Yang, L., Zhu, S., Wang, Y., & Shi, Y. (2024). Optimization of mechanical and antibacterial properties of SLM-fabricated TC4-5Cu alloy by annealing heat treatment. Journal of Alloys and Compounds, 971.

[23] Huang, S., Zhang, J., Ma, Y., Zhang, S., Youssef, S. S., Qi, M., et al. (2019). Influence of thermal treatment on element partitioning in α+β titanium alloy. Journal of Alloys and Compounds, 791, 575-585.

[24] Jamhari, F. I., Foudzi, F. M., Buhairi, M. A., Sulong, A. B., Mohd Radzuan, N. A., Muhamad, N., et al. (2023). Influence of heat treatment parameters on microstructure and mechanical properties of titanium alloys in LPBF: A short review. Journal of Materials Research and Technology, 24, 4091-4110.

[25] Meng, M., Yang, H., Fan, X. G., Yan, S. L., Zhao, A. M., & Zhu, S. (2017). Modeling of diffusion-controlled growth of primary α in heat treatment of two-phase Ti-alloys. Journal of Alloys and Compounds, 691, 67-80.

[26] Zhao, Z.-Y., Li, L., Bai, P.-K., Jin, Y., Wu, L.-Y., Li, J., et al. (2018). Heat treatment effect on microstructure and hardness of TC4 titanium alloy produced by selective laser melting. Materials, 11(8).

[27] Qi, C., Yang, D., Yu, P., Li, Z., Li, H., Zhang, K., et al. (2022). Influence of heat treatment on microstructure and mechanical properties of TC4 fabricated by laser melting deposition. Metals and Materials International, 28(12), 3068-3079.

[28] Wu, D., Chen, M., Fan, R., Xiao, W., & Wu, Y. (2023). Parameter optimisation and compressive properties of the TC31 titanium alloy X-type lattice structure by superplastic forming/diffusion bonding. Archives of Civil and Mechanical Engineering, 23(2).

[29] Zhong, X., Deng, T., Xiao, W., Zhong, M., Lai, Y., & Ojo, O. A. (2023). Effect of minor Sc modification on the high-temperature oxidation behaviour of near-α Ti alloy. Corrosion Science, 217.

[30] Satko, D. P., Shaffer, J. B., Tiley, J. S., Semiatin, S. L., Pilchak, A. L., Kalidindi, S. R., et al. (2016). Effect of microstructure on oxygen-rich-layer evolution and its impact on fatigue life during high-temperature operation of α/β titanium. Acta Materialia, 107, 377-389.

[31] Deconinck, L., Villa Vidaller, M. T., Bernardo Quejido, E., Jägle, E. A., Depover, T., &

Verbeken, K. (2023). In-situ hydrogen embrittlement evaluation of as-built and heat-treated laser powder bed fused Ti-6Al-4V versus conventionally cold-rolled Ti-6Al-4V. Additive Manufacturing, 76.

[32] Qiu, C., Yue, S., Adkins, N. J. E., Ward, M., Hassanin, H., Lee, P. D., et al. (2015). Effect of processing conditions on strut structure and compressive strength of cellular lattice structures fabricated by selective laser melting. Materials Science and Engineering: A, 628, 188-197.

[33] Keaveney, S., Shmeliov, A., Nicolosi, V., & Dowling, D. P. (2020). Investigation of process by-products in selective laser melting of Ti6Al4V powder. Additive Manufacturing, 36.

[34] Li, P., Warner, D. H., Fatemi, A., & Phan, N. (2016). Critical assessment of the fatigue performance of additively manufactured Ti–6Al–4V and future directions for research. International Journal of Fatigue, 85, 130-143.

[35] Zhai, Y., Galarraga, H., & Lados, D. A. (2016). Microstructure, static properties and fatigue crack growth mechanisms in Ti-6Al-4V fabricated by additive manufacturing: LENS and EBM. Engineering Failure Analysis, 69, 3-14.

[36] Wang, W., Xu, X., Ma, R., Xu, G., Liu, W., & Xing, F. (2020). Influence of heat treatment temperature on microstructure and mechanical properties of titanium alloy fabricated by laser melting deposition. Materials, 13(18).

[37] AlMahri, S., Santiago, R., Lee, D.-W., Ramos, H., Alabdouli, H., Alteneiji, M., et al. (2021). Evaluation of the dynamic response of triply periodic minimal surfaces under high strain-rate compression. Additive Manufacturing, 46.

[38] Li, D., Qin, R., Chen, B., & Zhou, J. (2021). Analysis of mechanical properties of lattice structures with stochastic geometric defects in additive manufacturing. Materials Science and Engineering: A, 822.

[39] Rowe, R., Almeida, N., Prather, A., Beck, S., Palazotto, A. N., & Davami, K. (2024). Effects of a modified heat treatment on the quasi-static and dynamic behaviour of additively manufactured lattice structures. The International Journal of Advanced Manufacturing Technology, 133(3-4), 1699-1713.

[40] Dai, J., Zhu, J., Chen, C., & Weng, F. (2016). High-temperature oxidation behaviour and research status of modifications for improving the high-temperature oxidation resistance of titanium alloys and titanium aluminides: A review. Journal of Alloys and Compounds, 685, 784-798.

[41] Ouyang, P., Mi, G., Li, P., He, L., Cao, J., & Huang, X. (2018). Non-isothermal oxidation behaviour and mechanism of a high-temperature near-α titanium alloy. Materials, 11(11).

[42] Rajabi, A., Mashreghi, A. R., & Hasani, S. (2020). Non-isothermal kinetic analysis of high-temperature oxidation of Ti–6Al–4V alloy. Journal of Alloys and Compounds, 815.

[43] Zeng, S., Zhao, A., Jiang, H., Fan, X., Duan, X., & Yan, X. (2013). Cyclic oxidation

behaviour of Ti-6Al-4V alloy. Oxidation of Metals, 81(3-4), 467-476.